

ANALYSIS OF INCOMPRESSIBLE FLUID FLOW INSIDE A LID-DRIVEN CAVITY

Prithvi Ramesh

ANALYSIS OF INCOMPRESSIBLE FLUID FLOW INSIDE A LID-DRIVEN CAVITY

*Intern report submitted to
BITS-Pilani Goa
as part for the award of the degree*

of

Bachelor of Technology

by

Prithvi Ramesh

Under the guidance of

Prof. Manab Kumar Das

IIT Kharagpur



DEPARTMENT OF MECHANICAL ENGINEERING

BITS PILANI GOA

CERTIFICATE

This is to certify that the report entitled, **Incompressible Flow inside Lid-Driven Cavity**, submitted by **Prithvi Ramesh** to BITS-Pilani Goa is a record of bona fide internship work under my supervision.

Dr. Manab Kumar Das
Professor
Mechanical Engineering
Department
Indian Institute of Technology
Kharagpur, 721302

I certify that

1. The work contained in the thesis is original and has been done by myself under the general supervision of my supervisor(s).
2. The work has not been submitted to any other Institute for any degree or diploma.
3. I have followed the guidelines provided by the Institute in writing the thesis.
4. I have conformed to the norms and guidelines given in the Ethical Code of Conduct of the Institute.
5. Whenever I have used materials (data, theoretical analysis, and text) from other sources, I have given due credit to them by citing them in the text of the thesis and giving their details in the references.
6. Whenever I have quoted written materials from other sources, I have put them under quotation marks and given due credit to the sources by citing them and giving required details in the references.

Contents

Certificate	i
Declaration	iii
List of figures	vii
Nomenclature	ix
Abstract	ix
1 Transient Lid Driven Cavity Flow	1
1.1 Introduction	1
1.1.1 Navier-Stokes Equation	1
1.1.2 Incompressible Flow	1
1.2 Case Setup	2
1.2.1 Grid	2
1.2.2 Boundary Conditions	2
1.2.3 The PISO Algorithm	3
1.2.4 Finite Volume Method	3
1.3 Post Processing	4
1.4 Results for Two Dimensional Cavity	5
1.4.1 Reynolds Number-100	6
1.4.2 Reynolds Number-400	8
1.4.3 Reynolds Number -1000	10
1.4.4 Reynolds Number -3200	12
1.4.5 Reynolds Number-5000	14
1.4.6 Reynolds Number - 7500	16
1.4.7 Reynolds Number - 10000	18
1.5 Results for Three Dimensional Cavity	20
1.5.1 Cubic Cavity	21

1.5.1.1	Reynolds Number -400	21
1.5.1.2	Reynolds Number -1000	21
1.5.1.3	Reynolds Number -2000	22
1.5.1.4	Reynolds Number -5000	22
1.5.2	Prismatic cavity	23
1.5.2.1	Reynolds Number -100	23
1.5.2.2	Reynolds Number -400	23
1.5.2.3	Reynolds Number 1000	24
1.5.2.4	Reynolds Number -2000	24
1.5.2.5	Reynolds Number -5000	25
1.6	Total Specific Kinetic Energy	25
Bibliography		28

List of Figures

1.1	Boundary Conditions for 2D square cavity	2
1.2	Vorticity formation	4
1.3	Streamlines	7
1.4	Streamlines	9
1.5	Streamlines	11
1.6	Streamlines	13
1.7	Streamlines	15
1.8	Streamlines	17
1.9	Streamlines	19
1.10	Comparison of x direction velocities along centerline for Square 2D cavity and Cubic 3D cavity	21
1.11	Comparison of x direction velocities along centerline for Square 2D cavity and Cubic 3D cavity	21
1.12	Comparison of x direction velocities along centerline for Square 2D cavity and Cubic 3D cavity	22
1.13	Comparison of x direction velocities along centerline for Square 2D cavity and Cubic 3D cavity	22
1.14	Comparison of x direction velocities along centerline for Rectangular 2D cavity and Prismatic 3D cavity of aspect ratio 2 each	23
1.15	Comparison of x direction velocities along centerline for Rectangular 2D cavity and Prismatic 3D cavity of aspect ratio 2 each	23
1.16	Comparison of x direction velocities along centerline for Rectangular 2D cavity and Prismatic 3D cavity of aspect ratio 2 each	24
1.17	Comparison of x direction velocities along centerline for Rectangular 2D cavity and Prismatic 3D cavity of aspect ratio 2 each	24

viii List of Figures

1.18 Comparison of x direction velocities along centerline for Rectangular 2D cavity and Prismatic 3D cavity of aspect ratio 2 each	25
1.19 Reynolds Number=100	26
1.20 Reynolds Number=1000	26
1.21 Reynolds Number=10000	27

ABSTRACT

Lid-Driven cavity is well-known benchmark problem in computational fluid dynamics (CFD). It is often used to validate new solvers since due to the plethora published data both experimental and computational . In this study a laminar OpenFOAM solver is used to study the velocity field obtained for Reynolds numbers of 100 , 400, 1000 , 2000 , 3200 , 5000 , 7500 and 10000. This wide range of Reynolds numbers allows a comprehensive analysis of the effect of viscosity on fluid flow patterns. The study included a two-dimensional square cavity and rectangular cavity, 3-dimensional prismatic cavity. The total specific kinetic energy for a low, intermediate and high Reynolds numbers is plotted along with time and variations are noted.

CHAPTER 1

Transient Lid Driven Cavity Flow

1.1 Introduction

1.1.1 Navier-Stokes Equation

The Navier-Stokes equations are a set of partial differential equations developed by the Swiss Mathematician Leonhard Euler in the 18th century and further improved by the British physicist Sir George Gabriel Stokes.

Continuity equation is ,

$$\partial \rho / \partial t + \nabla \cdot (\rho V) = 0 \quad (1.1)$$

Momentum equation :

$$\rho D U_i / D t = - \partial p / \partial x_i + \partial (\mu (\partial U_i / \partial x_j)) / \partial x_j + \partial / \partial x_i [(\lambda + \mu) \partial U_k / \partial x_k] + \rho B_i \quad (1.2)$$

Total acceleration = Pressure force + Viscous force + Force due to volumetric dilation + Body Force

1.1.2 Incompressible Flow

In continuum mechanics , incompressible flow or isochoric flow is the fluid flow in which the density is held constant or varies very slightly so that it is safe to assume it to be constant. Various flow phenomenon especially those involving a dense liquid can be modeled as incompressible which simplifies the setup and

2 Case Setup

decreases the computational time . Another way of representing incompressible flow is by putting the divergence of the flow velocity as zero. This result is obtained from the continuity equation.

$$\nabla \cdot u = 0 \quad (1.3)$$

1.2 Case Setup

1.2.1 Grid

The Grid was generated using the blockmeshDict files due to the simplicity of the geometry . Grading factors were used to increase cell concentration near the walls where the gradients are steeper. Due to the flow being globally laminar , the $y+$ values were not a consideration in determining grid size. The 2D grid used had a 120x120 cell count

1.2.2 Boundary Conditions

The top wall in all the geometries is given a tangential velocity of 1m/s and the other walls are given no-slip condition for velocity and symmetric (Gradient zero) for pressure.

The velocity and pressure were initialized with the zero components and magnitude respectively over the grid.

Given below is an illustration of the boundary conditions used.

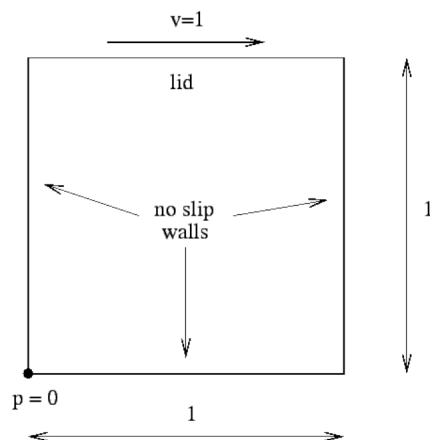


Figure 1.1: Boundary Conditions for 2D square cavity

1.2.3 The PISO Algorithm

The Pressure Implicit with Spiting (PISO) algorithm is a pressure-velocity coupled algorithm used for solving the Navier-Stokes set of equations when overall velocity and pressure profiles are unknown .The algorithm is a Finite Volume Method-based scheme that uses a staggered grid arrangement to avoid the formation of a 'checkerboard pressure field' which is a zigzag pressure filed , interpreted by the algorithm a uniform pressure field.

1. An initial pressure field initialised by the user is taken as the guessed pressure field (p^*) .
2. The momentum equation is then solved using this pressure field and the guessed velocities(U^*) at the cell faces (centre points of staggered grid) are obtained.
3. The corrected velocities designated as $U=U^*+U'$ are substituted into the continuity equations and a set of algebraic equations involving the velocity corrections are modified to include the pressure corrections (each velocity correction U' is expressed as a linear combination of the two adjutant cell centre's pressure corrections - p')
4. A corrected pressure field $p^{**} = p^* + p'$ is used to obtain a corrected velocity field as U^{**} through the momentum equations , these are then the new guessed velocity an pressure fields and the next set of corrections (U'' and p'') are obtained from the continuity equation . The sequence is looped till the corrections diminish below a threshold.

The PISO algorithm has an internal loop (unlike SIMPLE algorithm that uses an external loop) and due the fact that both the momentum and continuity equations are involved in every iteration , the velocity and pressure fields obtained at the end of each external loop are genuine . Due to this feature the PISO algorithm is highly suited for Transient flows.

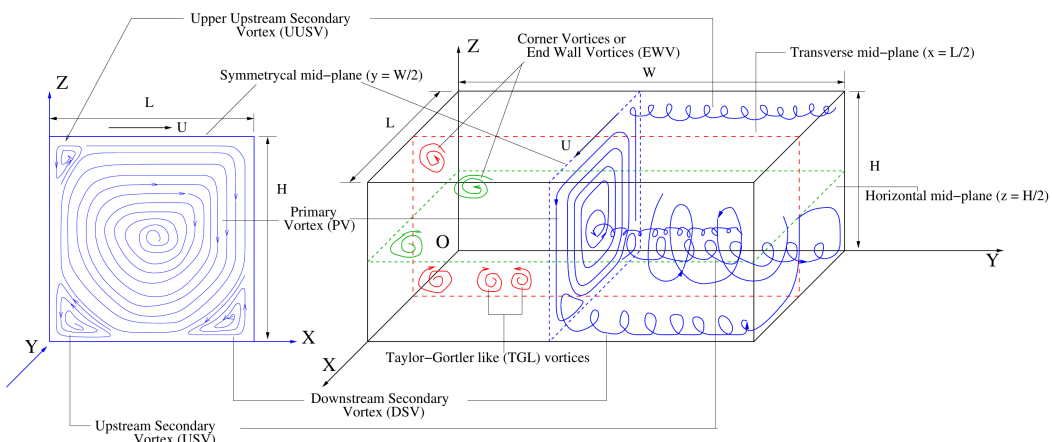
1.2.4 Finite Volume Method

The domain is divided into a number of non-overlapping control volumes such that there is one control volume surrounding each grid point. The differential equations are integrated over each control volume . Piece-wise linear profiles for the dependent variables within a control volume are used to evaluate the required integrals. The advantage of the control volume formulation is that the

resulting solution assures integral conservation of quantities such as mass, momentum and energy over the entire domain. The method can also easily be formulated for unstructured meshes since no assumption regarding the shapes of control volumes is made .OpenFOAM uses a cell-centroid approach for the solution like many other commercial CFD packages. The finite volume method is contrasted with finite difference method which only works for a grid with all nodes lying on two or three perpendicular axis like the 'x,y,z' coordinate system and extensive conversions are required for grids points that deviate from these axis , the finite volume method on the other hand does not require any conversions as such and can easily be applied for complex geometries .

1.3 Post Processing

Figure 1.2: Vorticity formation



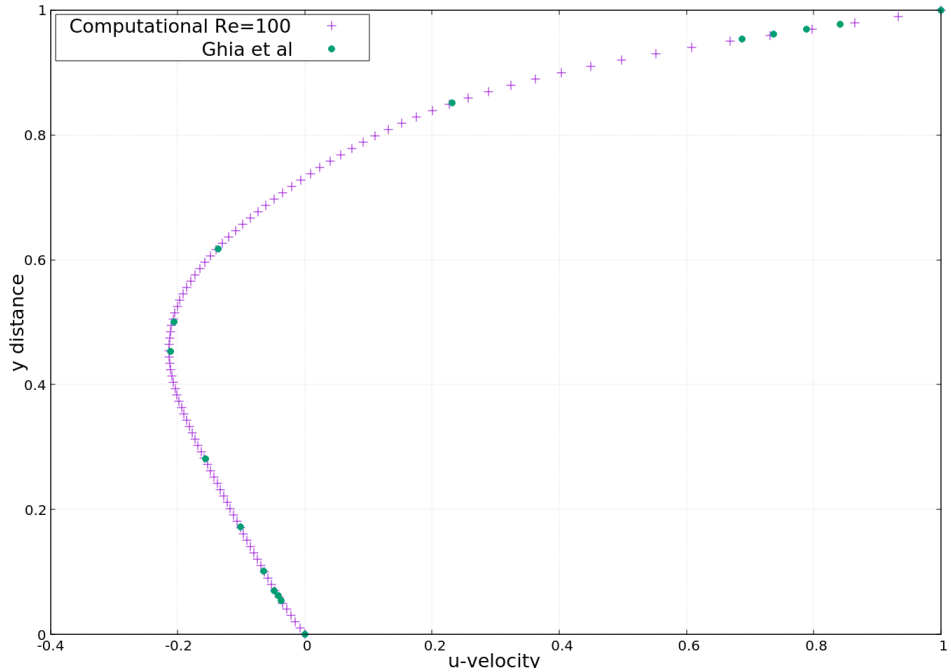
The results obtained are displayed in the form of streamlines, contours, and plots. The data was compared with the . The standard post-processing tool available with OpenFOAM - the paraView was used to obtain the streamlines and contours . To obtain the plots the foamGet command was used in conjunction with the singleGraph . Two separate start and end points were given , the first one was the horizontal line stretching through the geometric center , and the second was a vertical case again passing through the geometric center. For the vertical line y-component or 'v' of the velocity was used , and for the horizontal line the x-component or the 'u' velocity was used. Based on the results obtained in the singleGraph.

1.4 Results for Two Dimensional Cavity

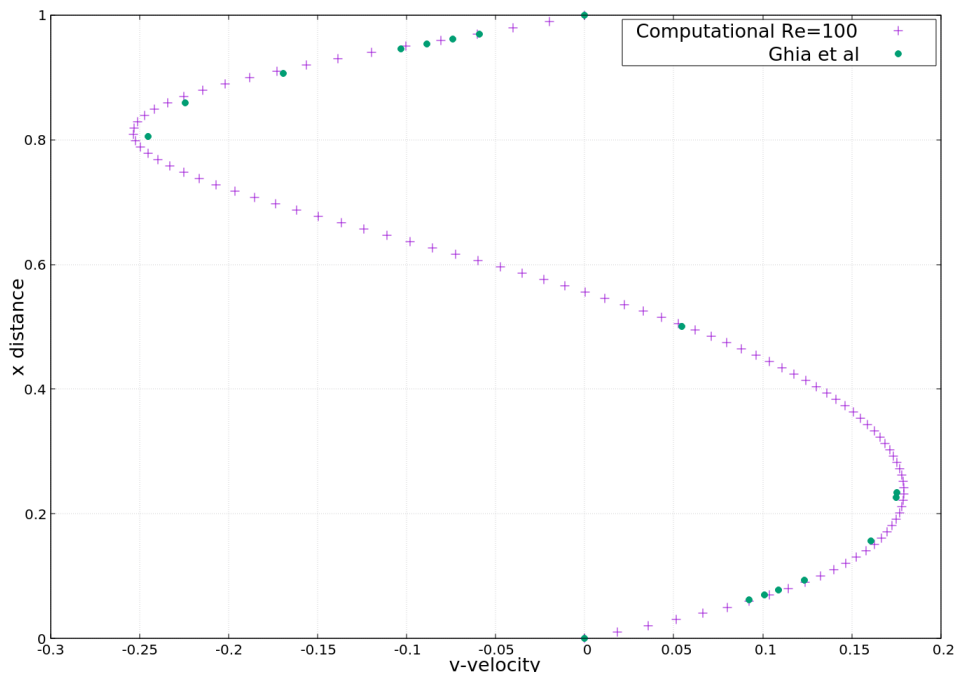
The results of the simulations which were run with a time step of 0.005 seconds are compared with the published data of Ghia et al(1982)[4] . The first three cases had a end time of 270 seconds to reach reach convergence. The Reynolds numbers of 3200 up to 7500 were run for 500 seconds and for Reynolds number of 10000- convergence was observed after 4000 seconds

1.4.1 Reynolds Number-100

Being a lower Reynolds number case very little or no formation of eddies was observed. Due to relatively higher viscosity the momentum diffusivity of the flow is larger and the lid velocity (of magnitude 1) is seen to be penetrating deeper into the domain . This penetration reduces for high Reynolds number cases.



(a) Comparison of u-velocity along cavity height



(b) Comparison of v-velocity along cavity length

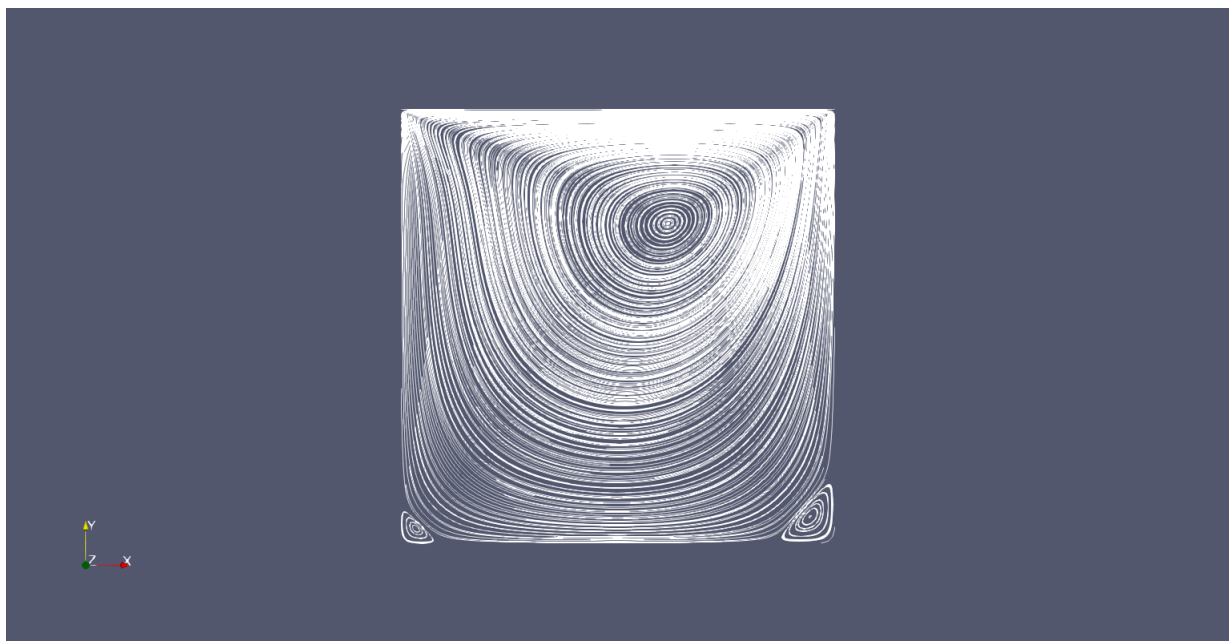
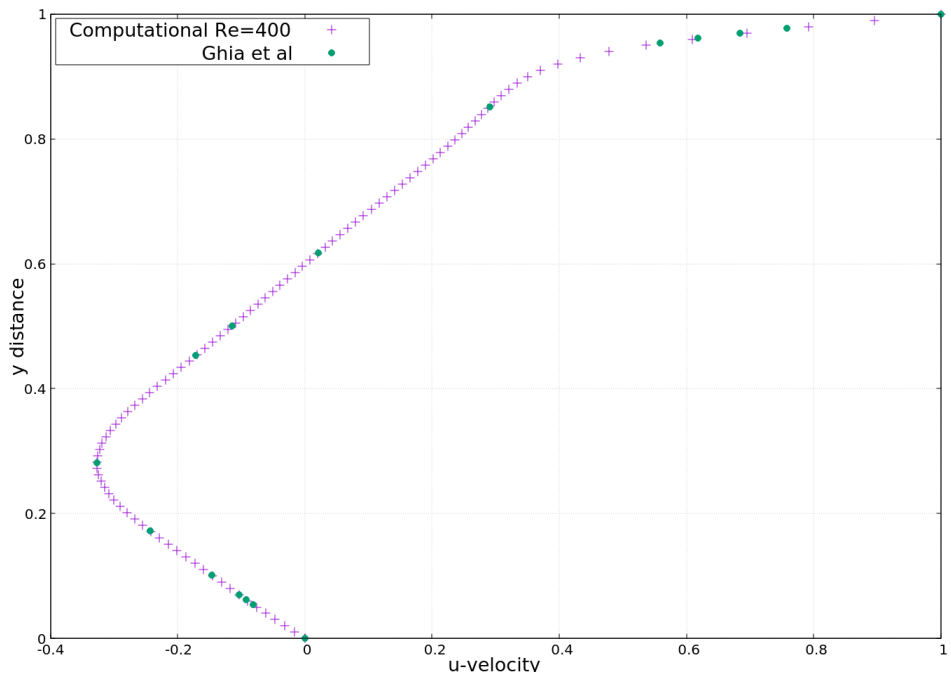


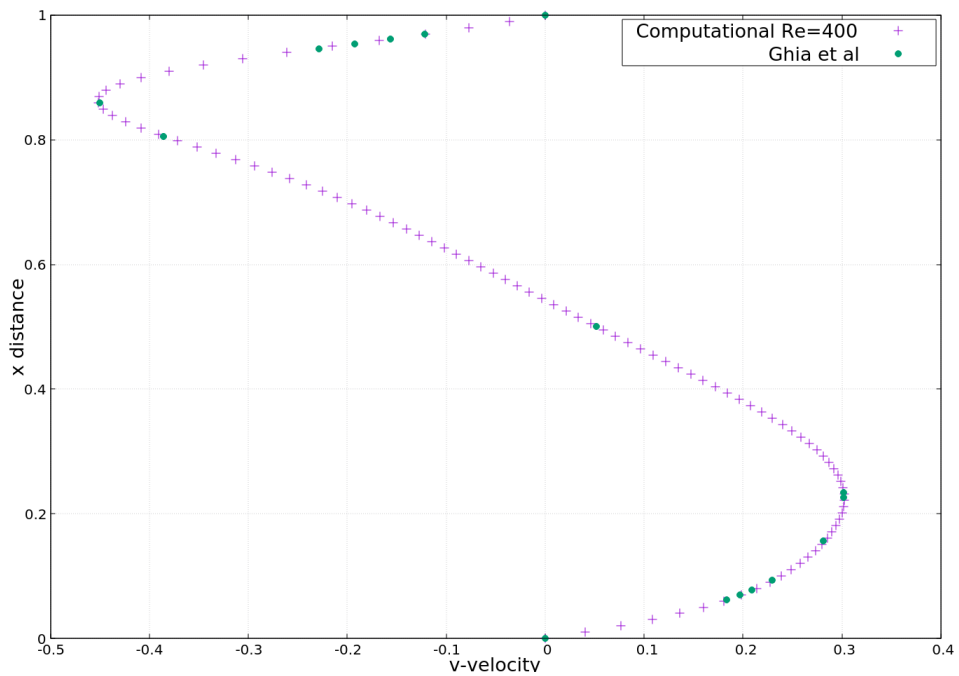
Figure 1.3: Streamlines

1.4.2 Reynolds Number-400

No eddy formation was observed . Larger velocities were observed near the center of the geometry.



(a) Comparison of u-velocity along cavity height



(b) Comparison of v-velocity along cavity length

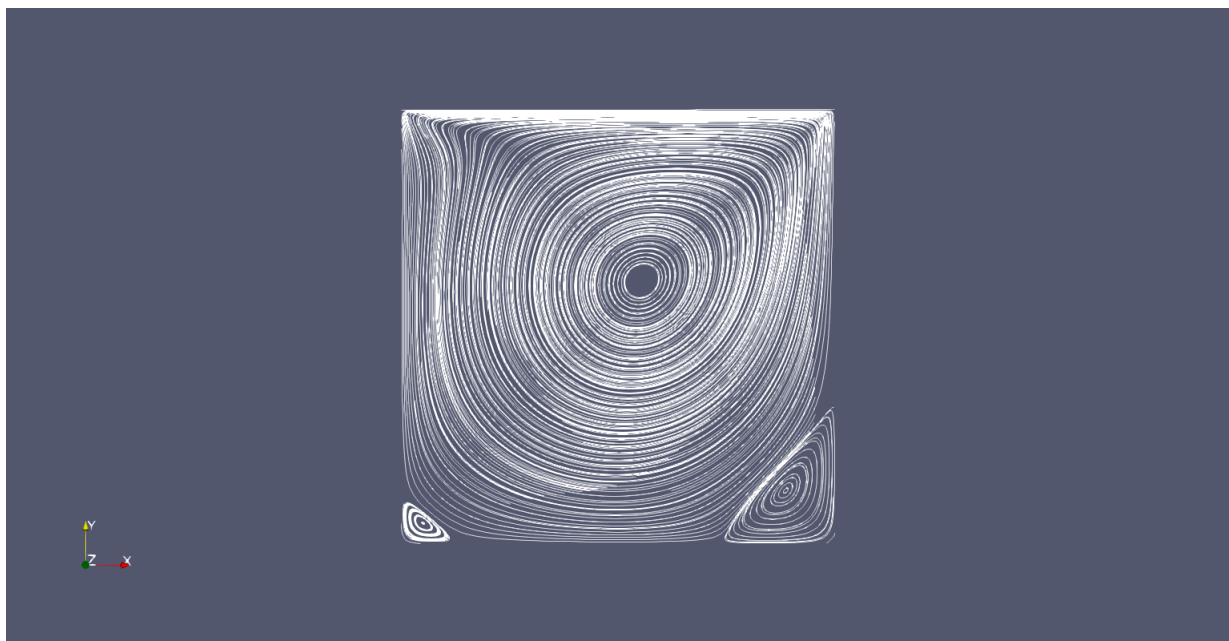
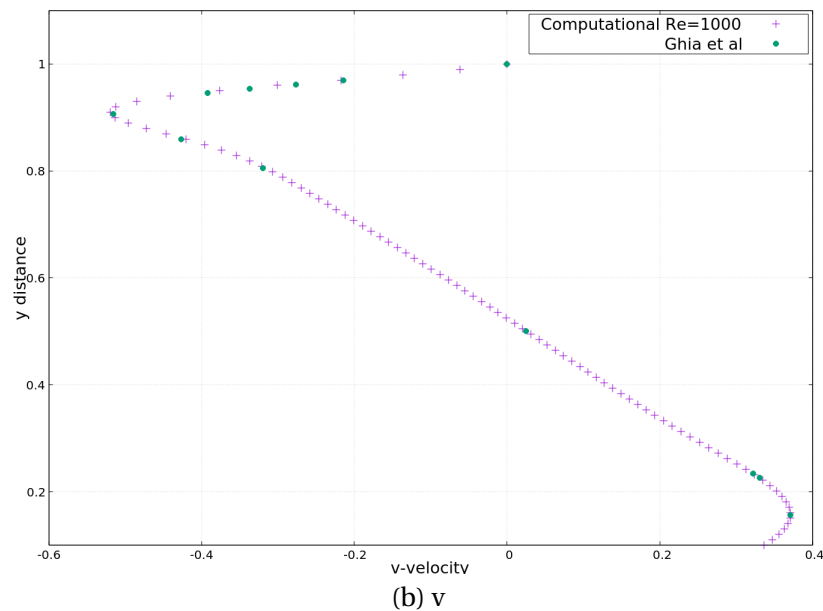
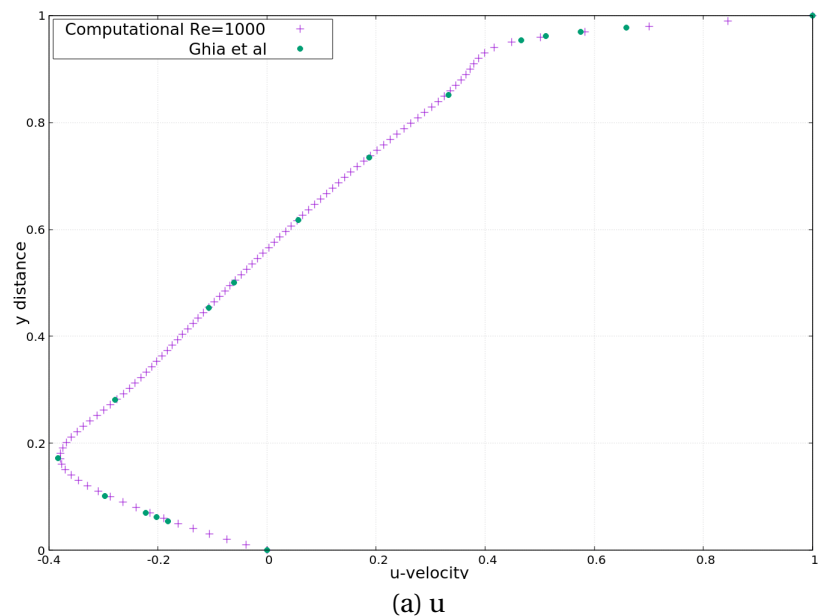


Figure 1.4: Streamlines

1.4.3 Reynolds Number -1000

Eddy formation was observed at the lower left and right corners.



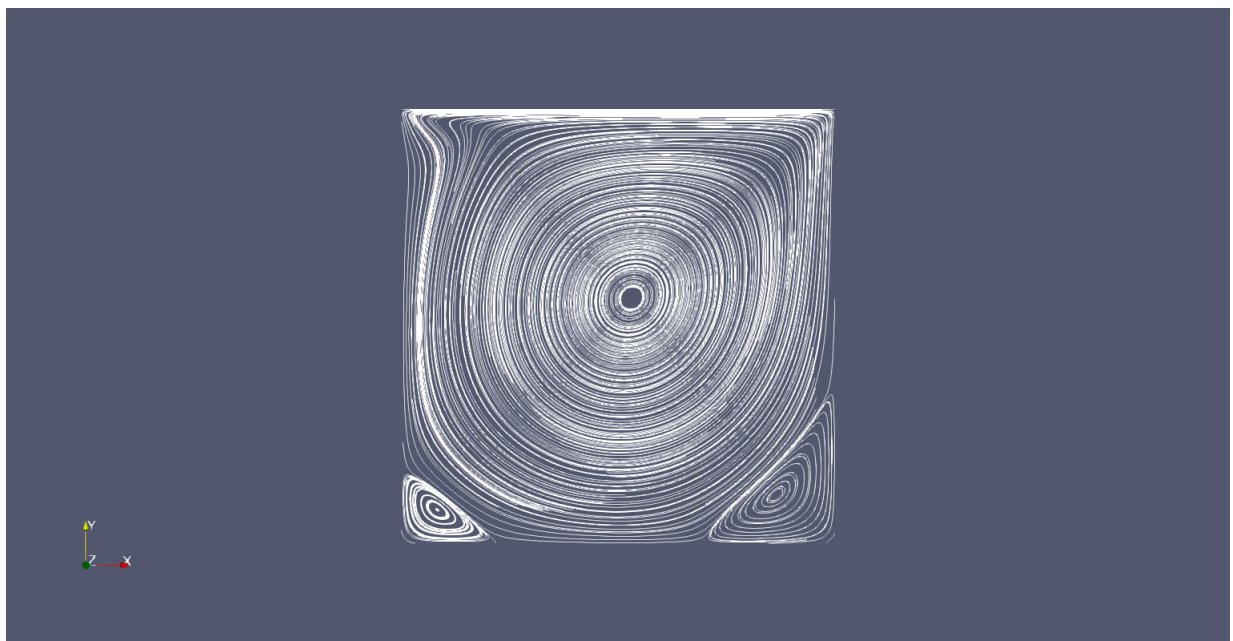
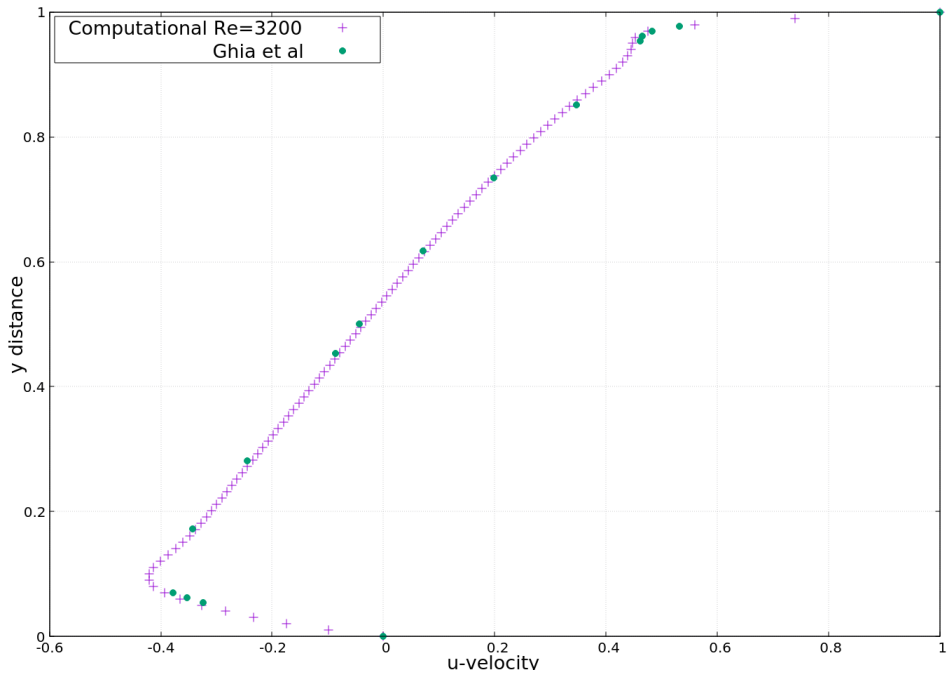


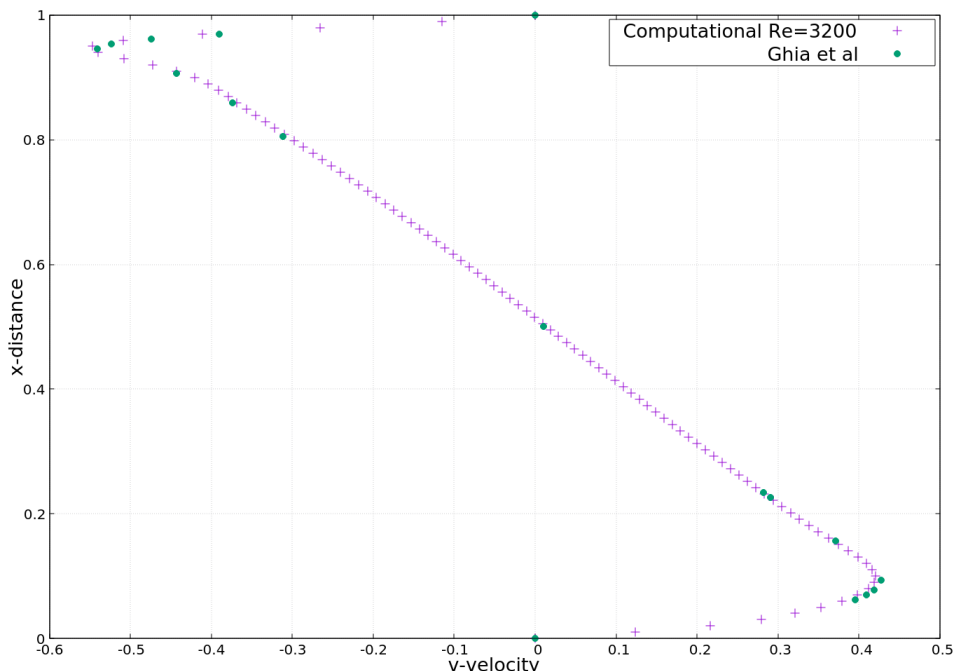
Figure 1.5: Streamlines

1.4.4 Reynolds Number -3200

Due to the increase in Reynolds number and the subsequent reduction in the dynamic viscosity the contribution of the convective term is more than the diffusion term in the Navier-Stokes equation . This results in longer time needed for the boundary information to reach the center of the domain. Significant eddy formation was observed on the lower left and right corners and the top left corner of the domain.



(a) Comparison of u-velocity along cavity height



(b) Comparison of v-velocity along cavity length

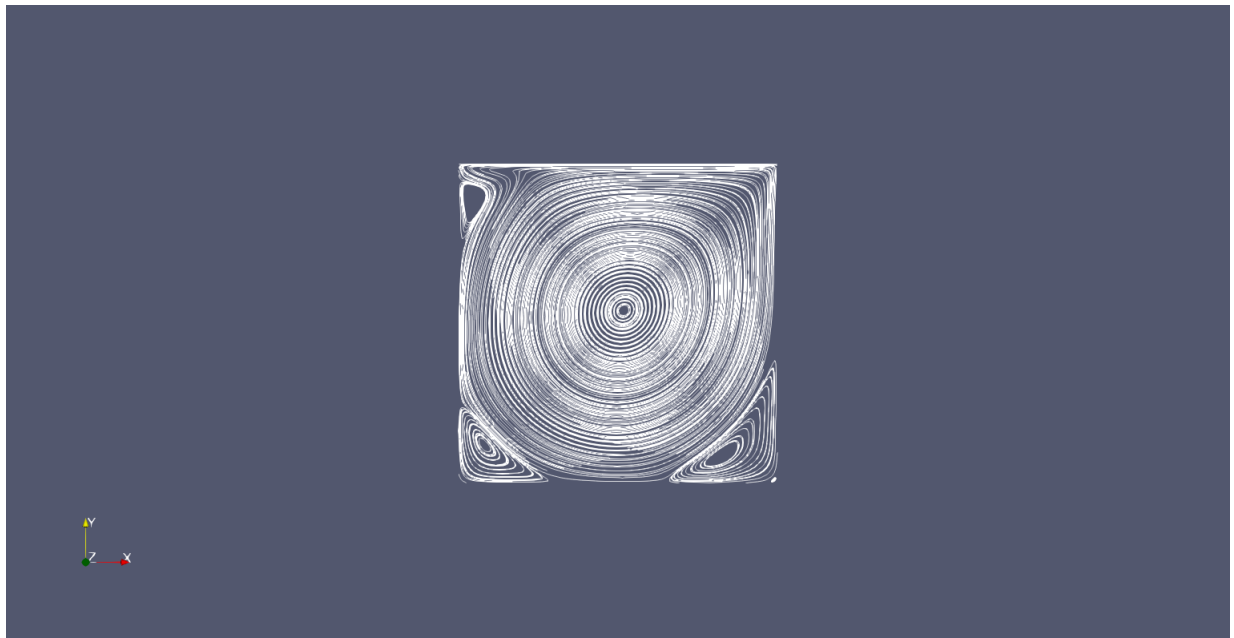
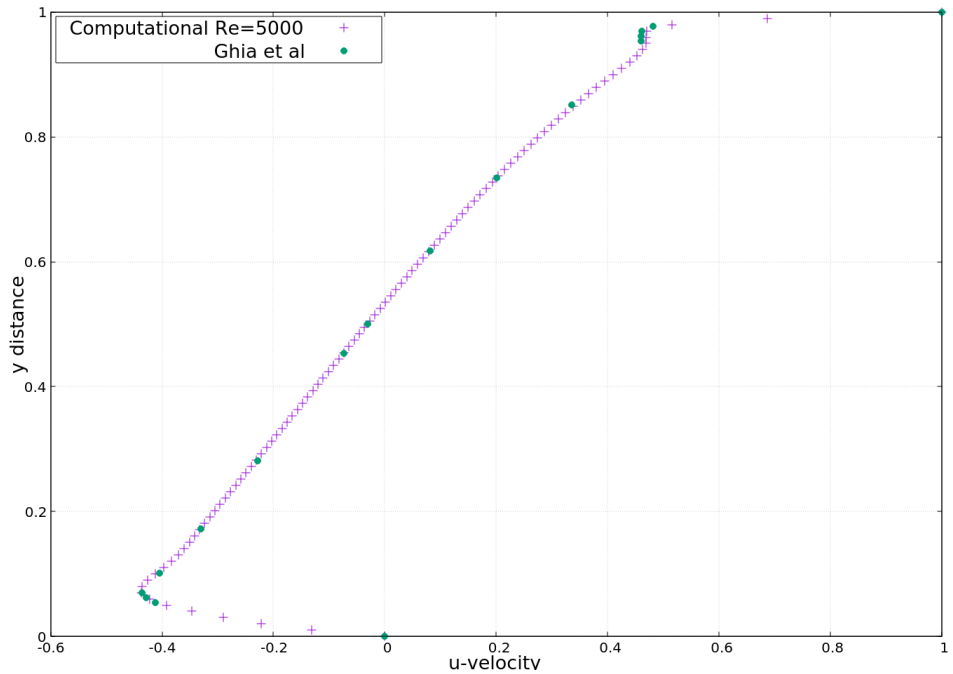


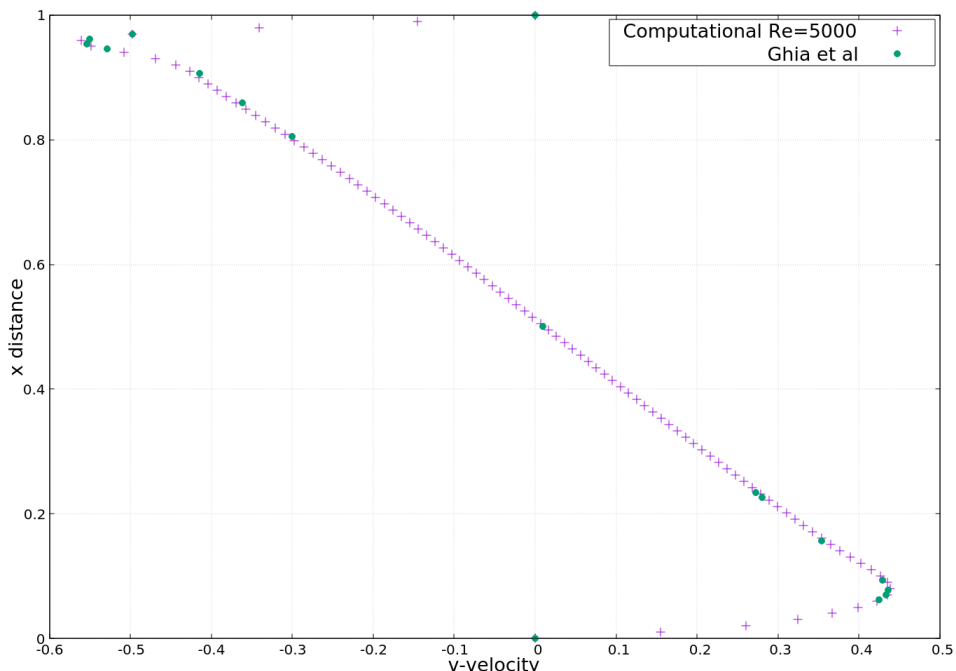
Figure 1.6: Streamlines

1.4.5 Reynolds Number-5000

Eddy formation was observed on the top , left and right corners of the domain. Results obtained are in close agreement with Ghia et al(1982) [4], however deviation are being observed close to the upper shearing lid , due to the steep velocity gradients.



(a) Comparison of u-velocity along cavity height



(b) Comparison of v-velocity along cavity length

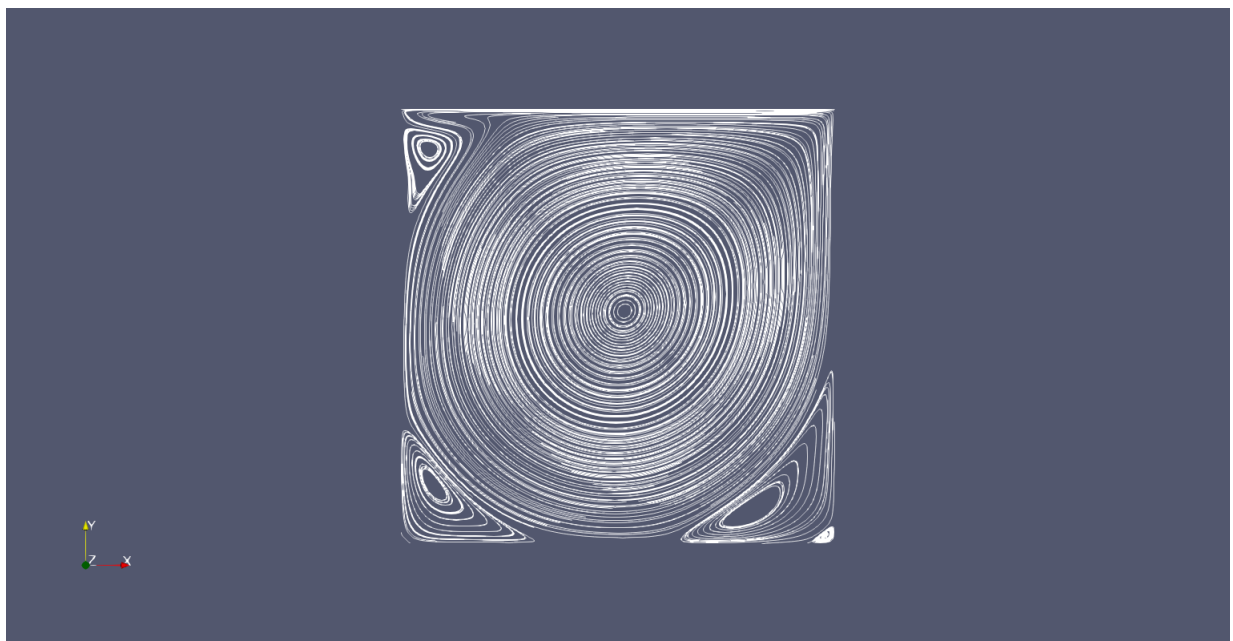
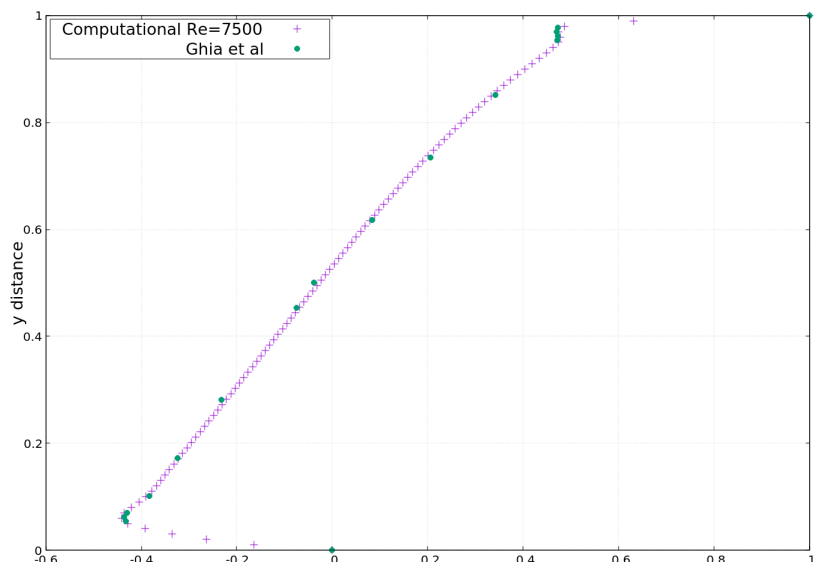


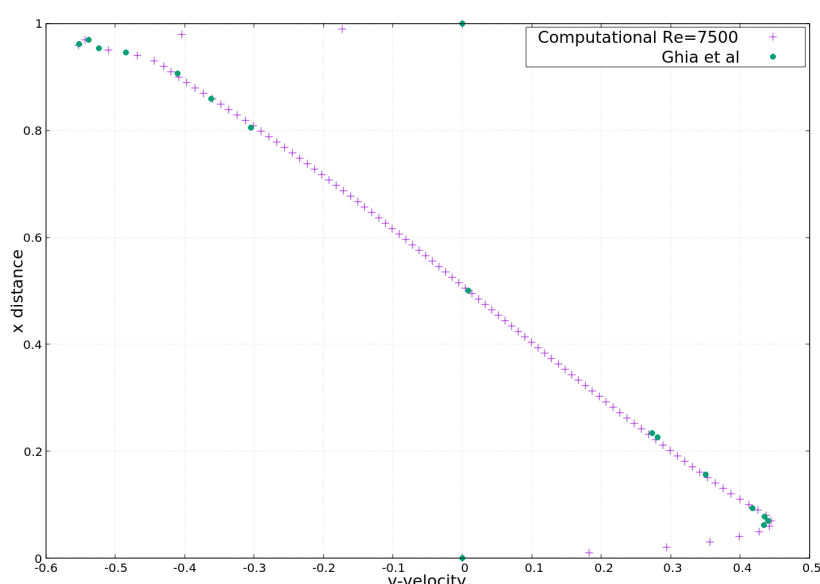
Figure 1.7: Streamlines

1.4.6 Reynolds Number - 7500

Eddy formation was observed in the top , left and right corners. The results are in close agreement with Ghia et al(1982) [4],however slight deviations are being observed near the top moving wall.



(a) Comparison of u-velocity along cavity height



(b) Comparison of v-velocity along cavity length

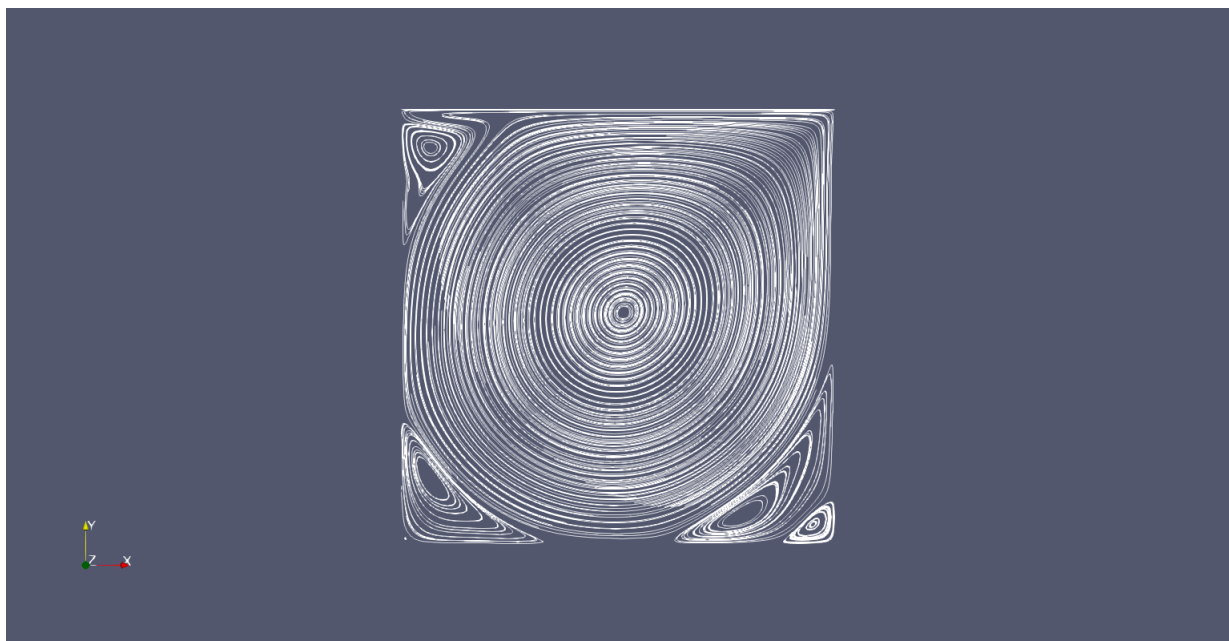
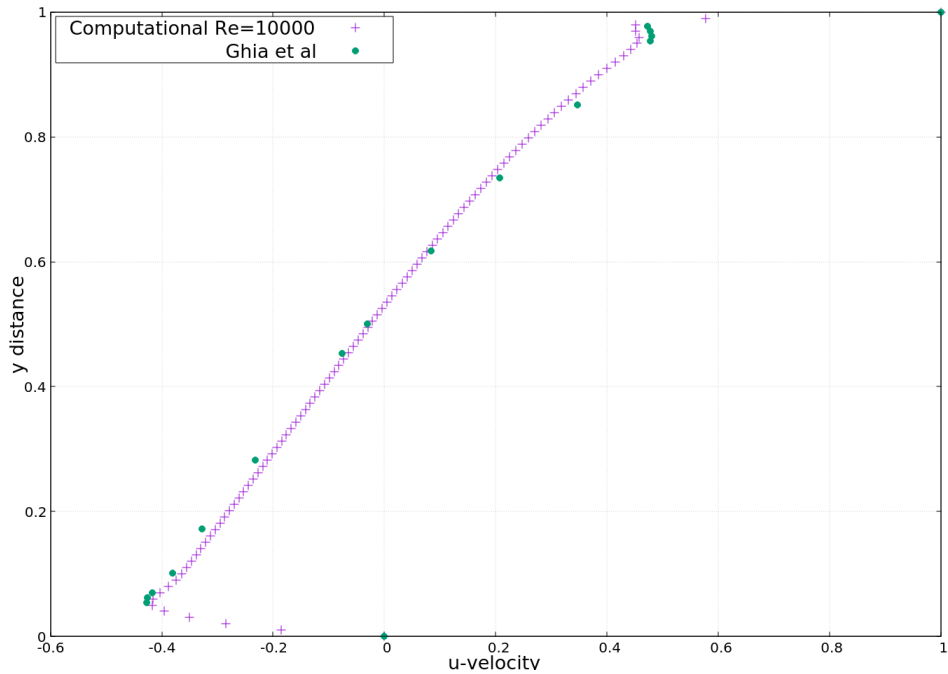


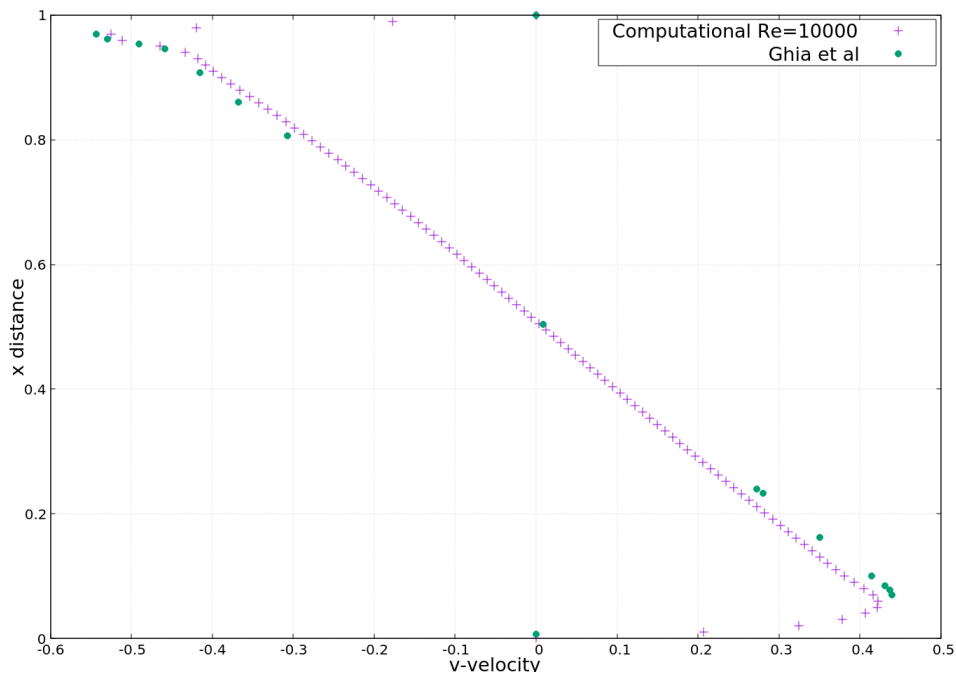
Figure 1.8: Streamlines

1.4.7 Reynolds Number - 10000

The reduced viscosity resulted in significantly longer time taken for the boundary information to reach the center. Due to this reason , the final result displays higher deviation from the published results than the lower Reynolds number cases .



(a) Comparison of u-velocity along cavity height



(b) Comparison of v-velocity along cavity length

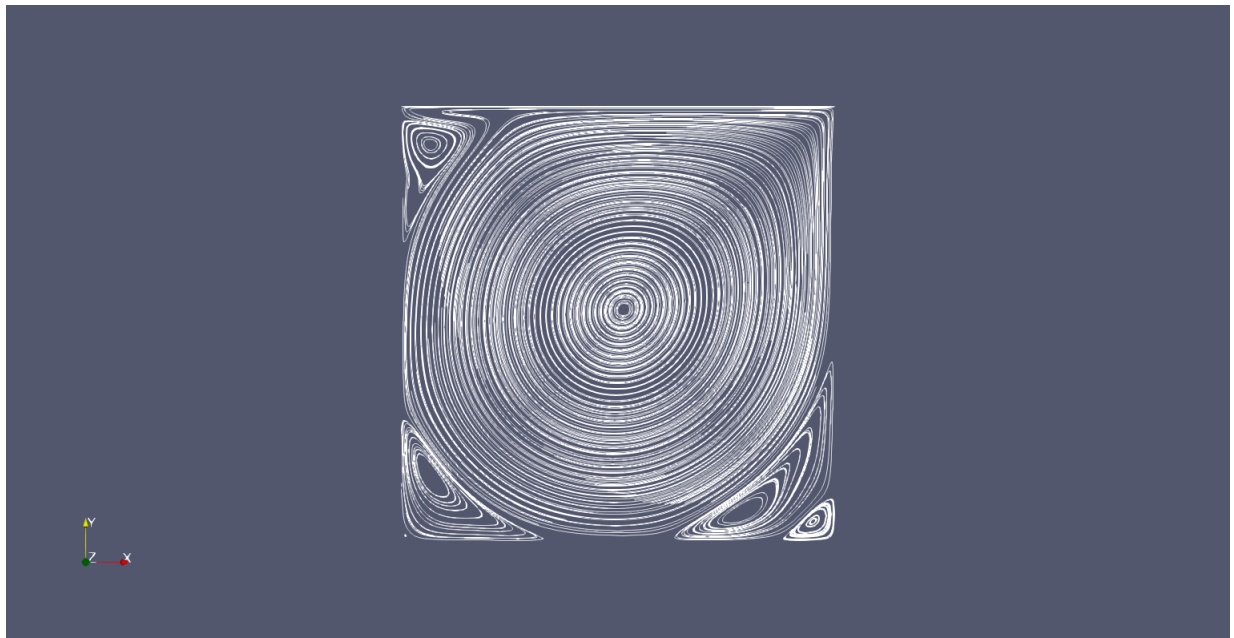


Figure 1.9: Streamlines

1.5 Results for Three Dimensional Cavity

The cubic cavity is a 3-Dimensional analogue of the square problem . The solution for the 3D cubic and prismatic cavities are computationally expensive and therefore a 20x20x20 grid is used . A mesh dependence test was preformed and the grid was found to be satisfactory .The grid is also stretched to allow for higher resolution near the walls(Faces) where the velocity gradients are large .Steady state condition was obtained till a a Reynolds number of 5000. The boundary conditions are similar to the square cavity . Three components of the velocity are set zero on all faces with the exception of the top face where the x-component was set to 1. The graphs generated are compared with the same Reynolds numbered flow of 2D square cavity. A comparison of the results for similar Reynolds numbers has been drawn between the 2d and 3D results using the centreline velocities.

1.5.1 Cubic Cavity

1.5.1.1 Reynolds Number -400

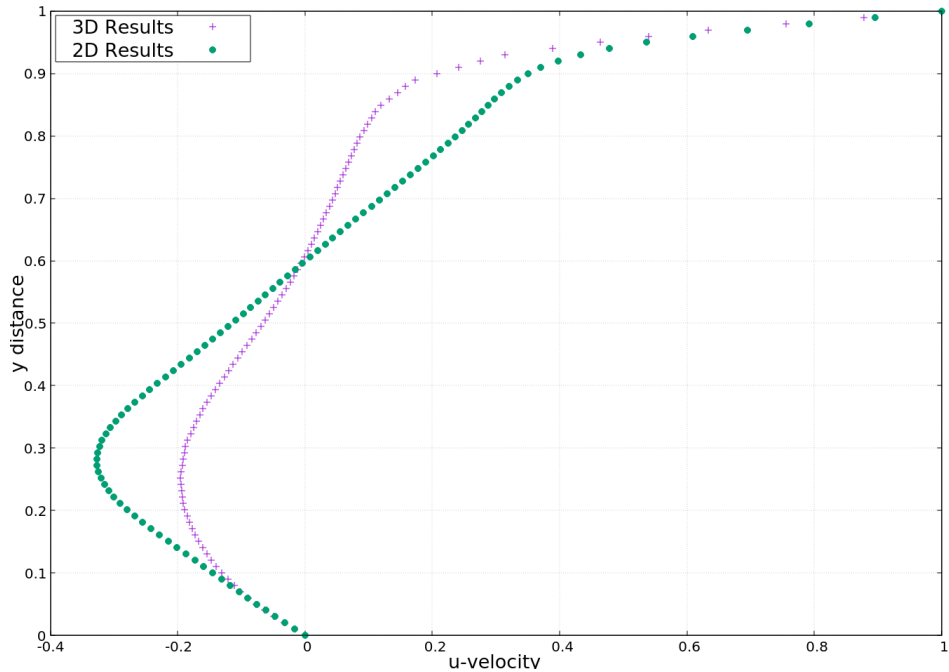


Figure 1.10: Comparison of x direction velocities along centerline for Square 2D cavity and Cubic 3D cavity

1.5.1.2 Reynolds Number -1000

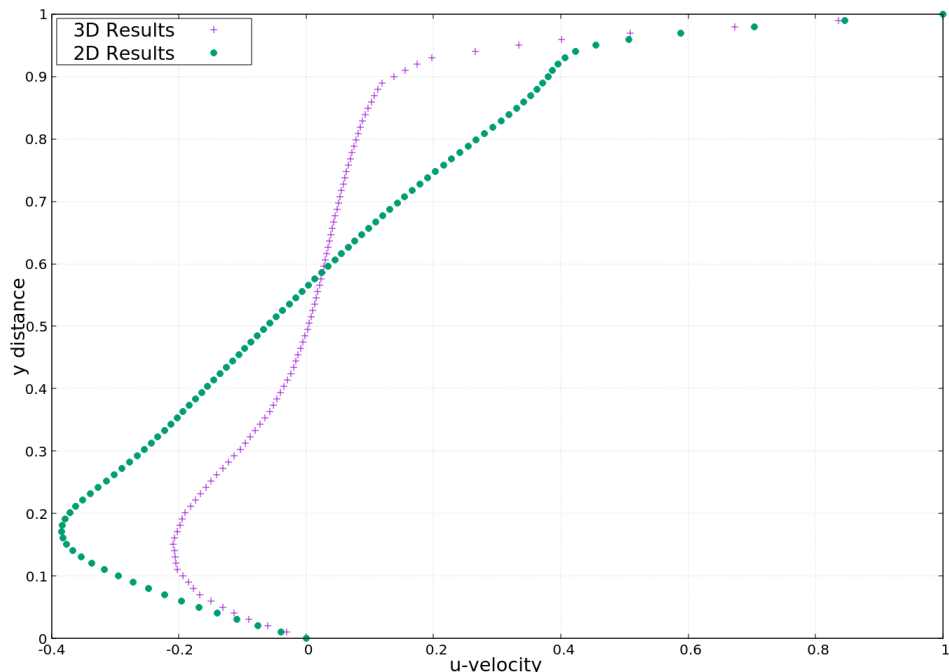


Figure 1.11: Comparison of x direction velocities along centerline for Square 2D cavity and Cubic 3D cavity

1.5.1.3 Reynolds Number -2000

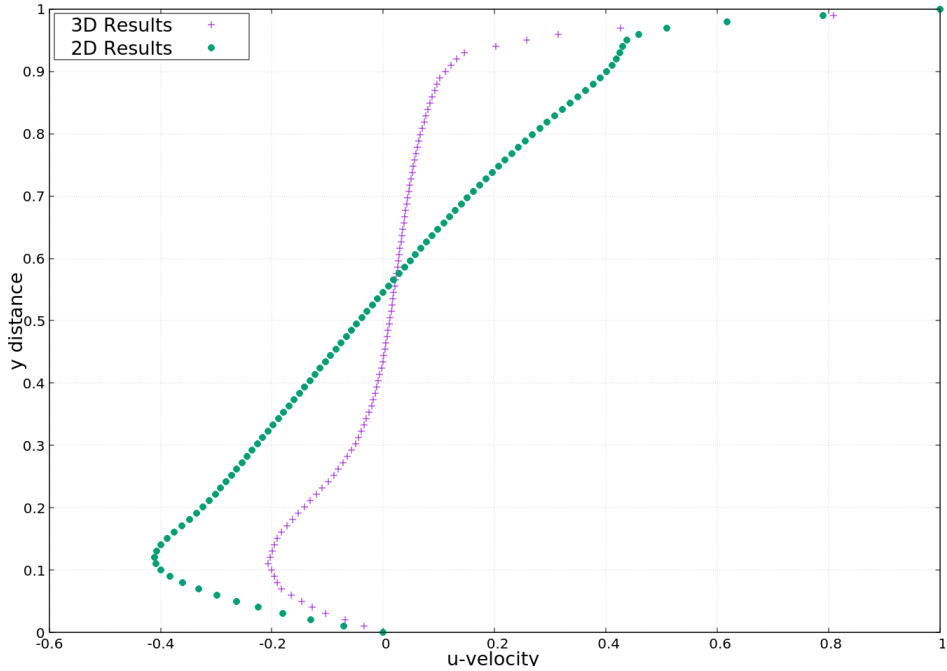


Figure 1.12: Comparison of x direction velocities along centerline for Square 2D cavity and Cubic 3D cavity

1.5.1.4 Reynolds Number -5000

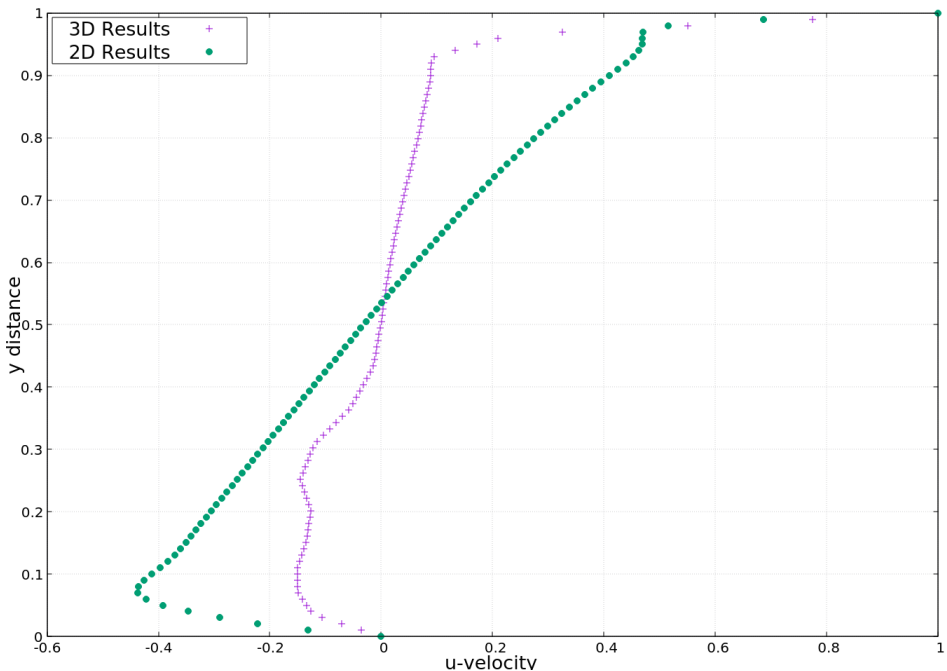


Figure 1.13: Comparison of x direction velocities along centerline for Square 2D cavity and Cubic 3D cavity

1.5.2 Prismatic cavity

1.5.2.1 Reynolds Number -100

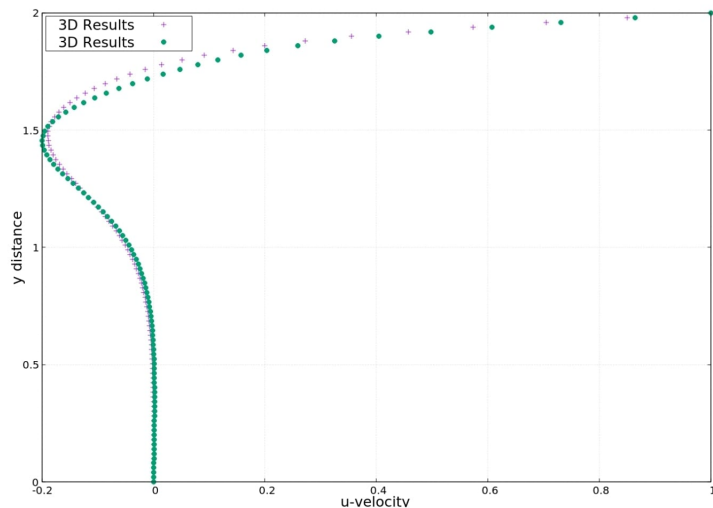


Figure 1.14: Comparison of x direction velocities along centerline for Rectangular 2D cavity and Prismatic 3D cavity of aspect ratio 2 each

1.5.2.2 Reynolds Number -400

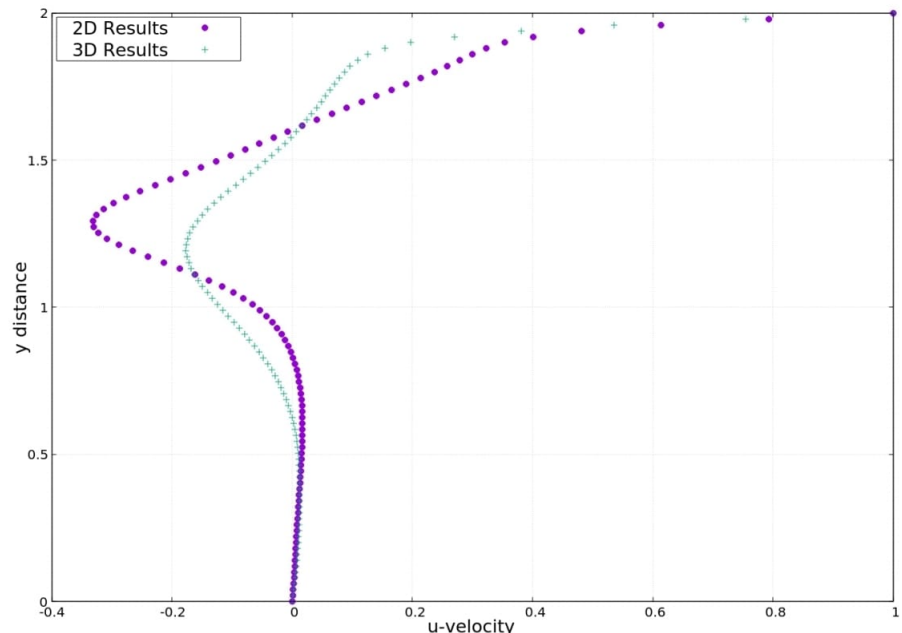


Figure 1.15: Comparison of x direction velocities along centerline for Rectangular 2D cavity and Prismatic 3D cavity of aspect ratio 2 each

1.5.2.3 Reynolds Number 1000

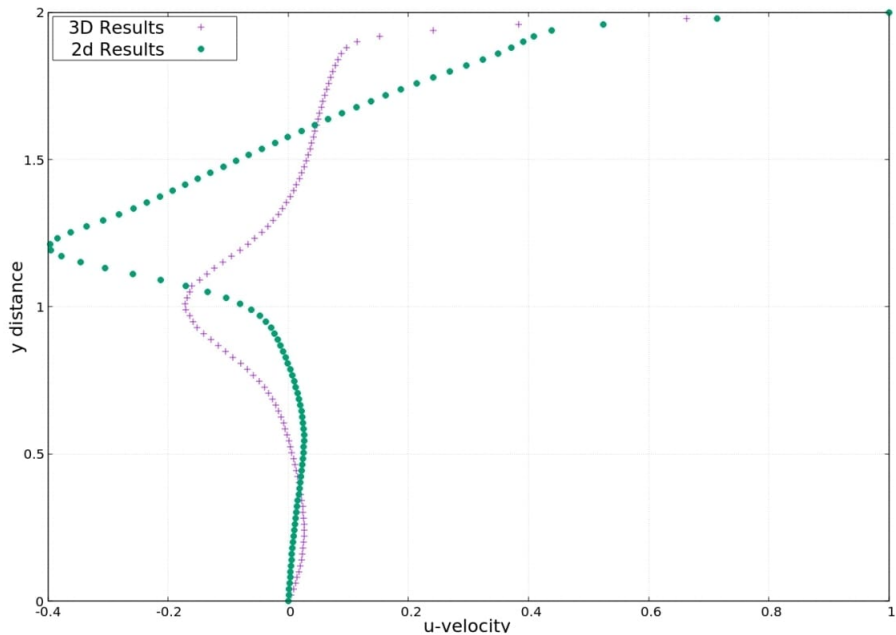


Figure 1.16: Comparison of x direction velocities along centerline for Rectangular 2D cavity and Prismatic 3D cavity of aspect ratio 2 each

1.5.2.4 Reynolds Number -2000

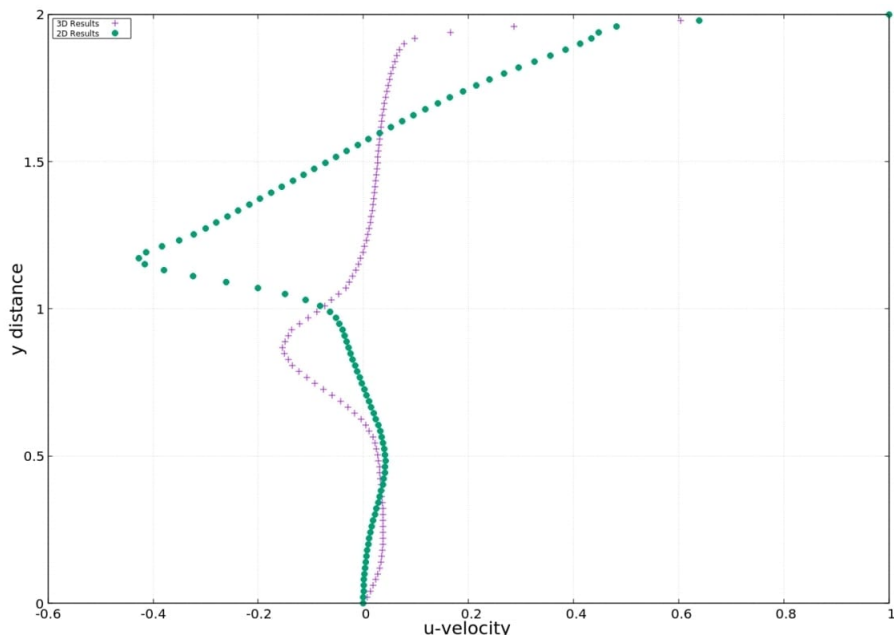


Figure 1.17: Comparison of x direction velocities along centerline for Rectangular 2D cavity and Prismatic 3D cavity of aspect ratio 2 each

1.5.2.5 Reynolds Number -5000

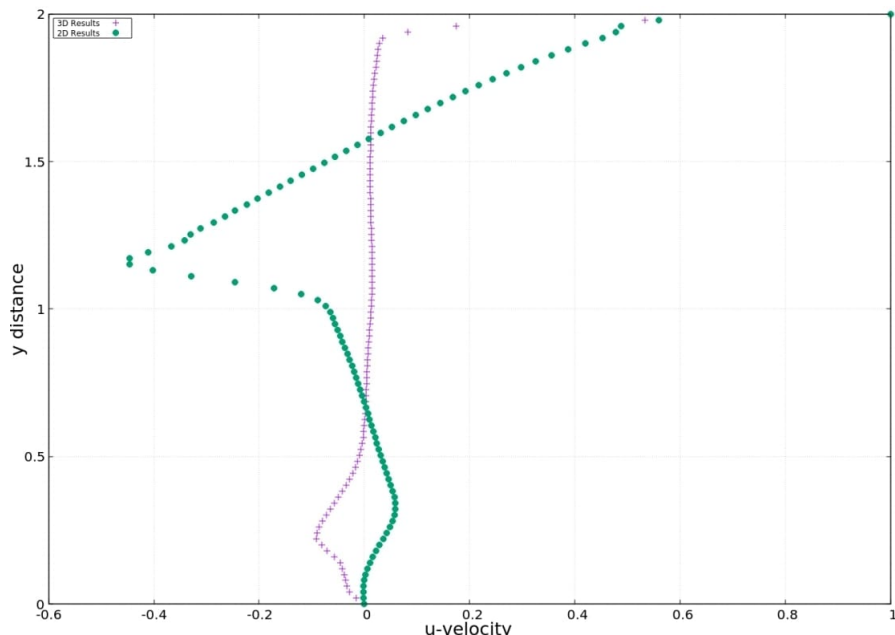


Figure 1.18: Comparison of x direction velocities along centerline for Rectangular 2D cavity and Prismatic 3D cavity of aspect ratio 2 each

1.6 Total Specific Kinetic Energy

The quality is obtained as the summation of the square of the velocity magnitude multiplied half and summed over all the cells included in the computational domain. The simulations are done for a 2-D rectangular cavity with aspect ratio as 2.

$$TKE = 0.5 * |U| * |U|$$

The values obtain are only taken for a relativistic comparison of the velocity patterns and the effect of viscosity on them and are not reflective of the true kinetic energy possessed by the fluids since the mass term is excluded.

26 Total Specific Kinetic Energy

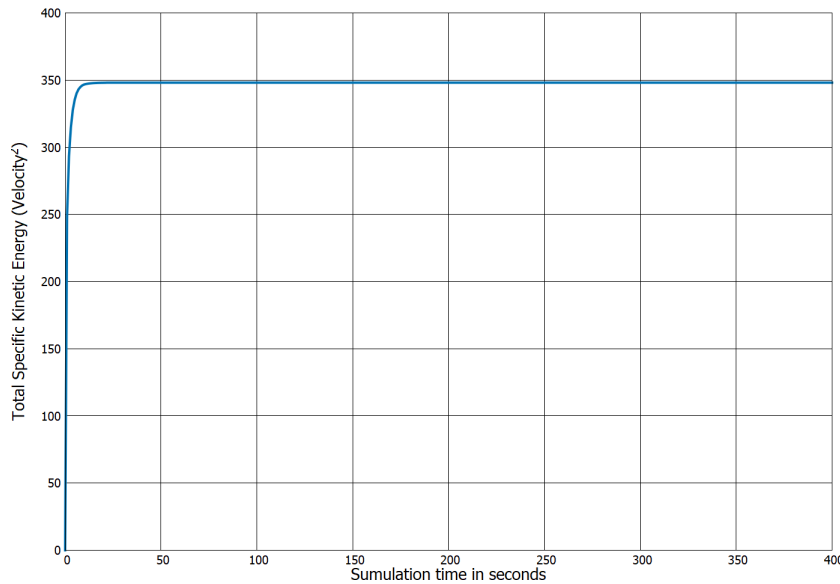


Figure 1.19: Reynolds Number=100

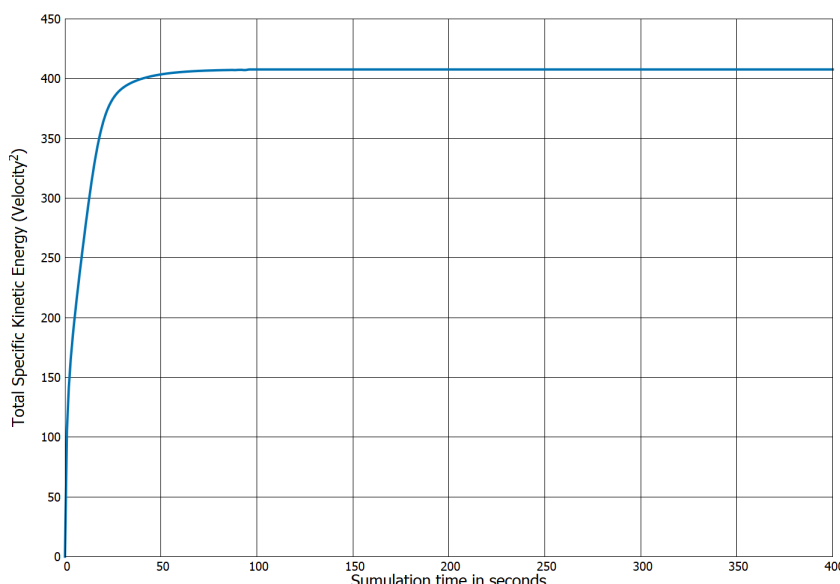


Figure 1.20: Reynolds Number=1000

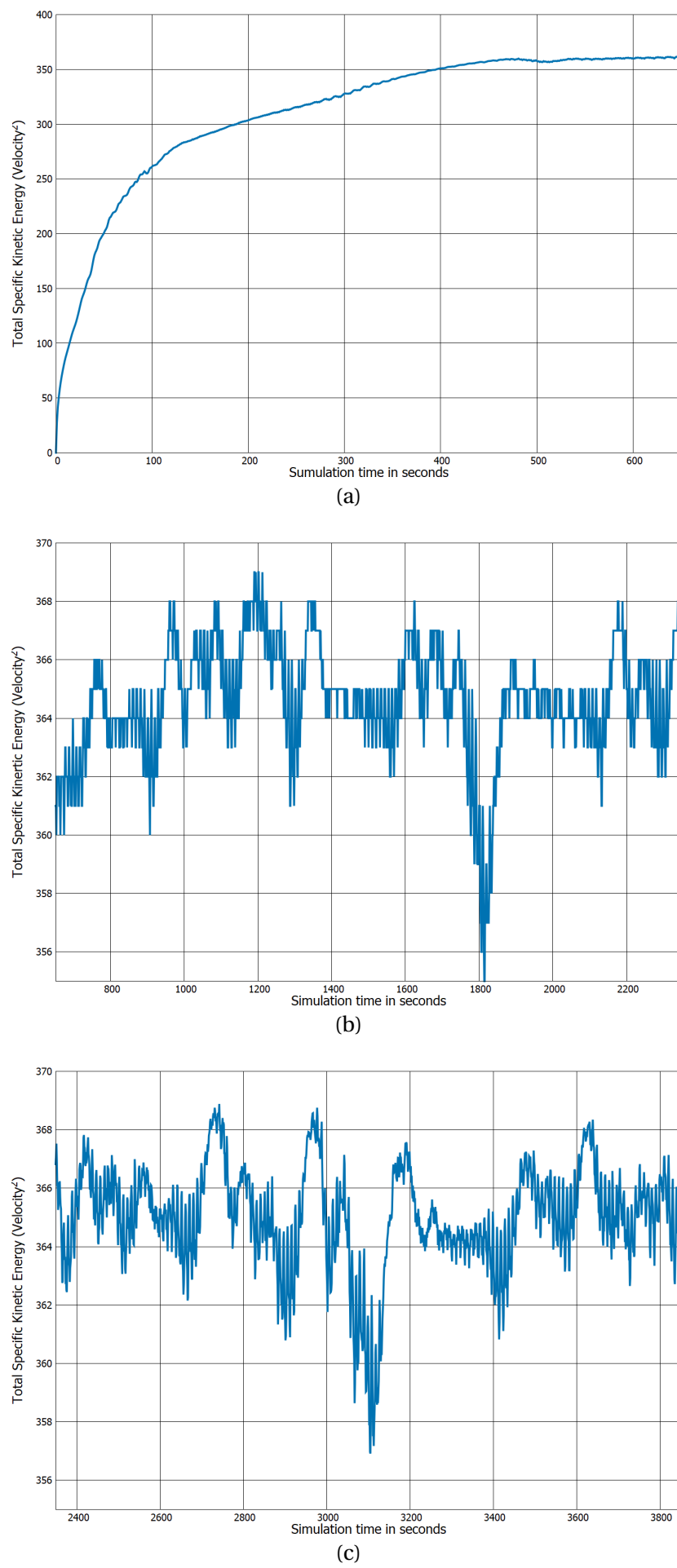


Figure 1.21: Reynolds Number=10000

The analysis of the Total Specific Kinetic Energy indicates that the velocity values stabilize relatively early for lower Reynolds number. For higher Reynolds number, the velocity values stabilization takes longer since the boundary information takes longer to reach the cavity center due to the reduced viscosity, further the high Reynolds number case has the velocity values fluctuating continuously.

Bibliography

- [1] T. Chiang and T. W. H. Sheu. A numerical revisit of backward-facing step flow problem. *Physics of Fluids*, 11(4):862–874, 1999.
- [2] A. Cortes and J. Miller. Numerical experiments with the lid driven cavity flow problem. *Computers & Fluids*, 23(8):1005–1027, 1994.
- [3] L. Fuchs and N. Tillmark. Numerical and experimental study of driven flow in a polar cavity. *International Journal for numerical Methods in Fluids*, 5(4):311–329, 1985.
- [4] U. Ghia, K. N. Ghia, and C. T. Shin. High-Re solutions for incompressible flow using the Navier-Stokes equations and a multigrid method. 48:387–411, 1982.